

CHoKI-based MPC for blood glucose regulation in Artificial Pancreas with probabilistic constraints

Beatrice Sonzogno¹, José María Manzano², Marco Polver¹, Fabio Previdi¹ and Antonio Ferramosca¹

Abstract—This work presents a Model Predictive Control (MPC) algorithm for the Artificial Pancreas. In this work, we assume that an a-priori model is unknown and the Componentwise Hölder Kinky Inference (CHoKI) data-based learning method is used to make glucose predictions. A stochastic formulation of the MPC with chance constraints is considered to have a less conservative controller. The data collection and the testing of the proposed controller are performed by exploiting the virtual patients of the FDA-accepted UVA/Padova simulator. The simulation results are quite satisfying since the time in hypoglycemia is reduced.

I. INTRODUCTION

Type 1 Diabetes (T1D) is a metabolic disease that affects millions of people all over the world, characterized by the autoimmune destruction of the pancreatic beta cells, causing the absence of insulin. This results in high Blood Glucose (BG) levels and thus T1D patients require daily exogenous insulin, whose amount computation is the key-point to restore their euglycemic range (BG between 70 and 180 mg/dL), avoiding hyper-/hypo- glyceemic conditons [1].

The availability of Continuous Glucose Monitoring (CGM) sensors and of pumps for continuous subcutaneous insulin injections, has led to the Artificial Pancreas (AP) development. The AP tries to mimic the functioning of a healthy pancreas, exploiting two insulin actions: the basal (continuous delivery of small amounts to manage fasting periods) and the boluses (bigger amount injected at meal times to face carbohydrate ingestion or when the BG level is unexpectedly too high).

Model Predictive Control (MPC) is among the most used algorithm for the AP, thanks to its ability to forecast future BG values. In MPC the control action is obtained by solving online, at each sampling time, a finite horizon optimal control problem. This way, MPC is able to compute the sequence of the best control actions (with length equal to the prediction horizon), minimizing a cost function and satisfying the constraints, in order to reach the desired goal. Then, the first control action is applied to the system and the procedure is

repeated at the following time step, in a receding horizon fashion [2].

MPC requires a model of the system to make predictions. Data-driven techniques may help to learn the behaviour of the systems directly from past data. The use of MPC as a control algorithm for the AP has been widely studied [3], [4], [5], [6], [7], [8], [9], [10], [11], [12], [13], [14]. All these works are based on a model of the T1D patients (usually physiological-based models [8]) for predictions. However, the employed models may not correctly describe the specific patient's glucose-insulin dynamics, characterized by inter- and also intra-patients variability. In this work, the model is assumed to be unknown and the idea is to directly use the data from the patients to learn their behaviour and to build a personalized controller. Here, the chosen learning method is the Componentwise Hölder Kinky Inference (CHoKI), a non-parametric learning technique which has been proved valid to learn nonlinear dynamical systems, and which favours the design of robust MPCs that are stable by design [15].

A drawback of this technique is that the deterministic bounds obtained may be so conservative that they render an infeasible setup. For this reason, in [16], a truncated bound on the prediction error was used to obtain practical controllers. In this work, we propose to use a stochastic description of uncertainties and constraints. To account for the model-system mismatch, the approach proposed in [17] is employed, since it allows for a small probability of constraints violation.

To collect the data needed for learning and to test the proposed control algorithms, the virtual patients of the UVA/Padova simulator [18] are exploited. This is a simulator accepted by the FDA as a substitute for preclinical trials.

The outline of the note is as follows: in Section II the CHoKI method is explained and applied to the T1D patient case. In Section III the MPC design is presented. In Section IV the chance constraints theory is shown and used in the MPC problem. Section V shows the results of the application of the proposed MPC on the UVA/Padova simulator. Section VI concludes the work.

Notation: A set of integers $[a, b]$ is denoted \mathbb{I}_a^b , \mathbb{R}^n is the set of real vectors of dimension n and $\mathbb{R}^{n \times m}$ is the set of real $n \times m$ matrices. Given $v, w \in \mathbb{R}^{n_v}$, the notation (v, w) implies $[v^T, w^T]^T$ and $v \leq w$ implies that the inequality holds for every component. $\|v\|$ stands for the Euclidean norm of v and $|v| = \{w : w_i = |v_i|, \forall i\}$. Given two sets A, B , $A \ominus B$ denotes the Pontryagin difference. Their Cartesian product is denoted $A \times B = \{(x, y) | x \in A, y \in B\}$. The box $\mathbb{B}(v) \subset \mathbb{R}^{n_v}$ is defined as $\mathbb{B}(v) = \{y : |y| \leq v\}$. An n, m -dimensional

¹ Department of Management, Information and Production Engineering, University of Bergamo, 24044 Dalmine, Bergamo, Italy

² Department of Engineering, Universidad Loyola Andalucía, 41704 Dos Hermanas, Seville, Spain

* This work was funded by the National Plan for NRRP Complementary Investments (PNC, established with the decree-law 6 May 2021, n. 59, converted by law n. 101 of 2021) in the call for the funding of research initiatives for technologies and innovative trajectories in the health and care sectors (Directorial Decree n. 931 of 06-06-2022) - project n. PNC0000003 - AdvANced Technologies for Human-centrEd Medicine (project acronym: ANTHEM). This work reflects only the authors' views and opinions, neither the Ministry for University and Research nor the European Commission can be considered responsible for them.

matrix of ones is denoted $\mathbb{1}_{n \times m}$. $[A]_j$ and $[a]_j$ define the j -th row and entry of the matrix A and vector a , respectively. The notation $\mathbb{P}_k\{\mathcal{A}\} = \mathbb{P}_k\{\mathcal{A}|x_k\}$ denotes the conditional probability of an event \mathcal{A} given the realization of x_k .

II. PROBLEM STATEMENT

Glucose level in T1D patients can be represented as sampled continuous-time system, described by an a-priori unknown discrete-time model, with the measured output $y(k) \in \mathbb{R}^{n_y}$ and the input $u(k) \in \mathbb{R}^{n_u}$. The goal in this case, as in the AP currently on the market, is to manage the basal insulin in an automatic fashion, while the postprandial boluses are assumed to be delivered manually. Thus, only the relation among BG, meals and basal insulin is considered. This means that there is one measurable output ($n_y = 1$), which is the BG level, in mg/dL, and there are two inputs ($n_u = 2$): a non-controllable one, which is the carbohydrates of the meals (u_1 , in mg) and a controllable one, which is the basal insulin (u_2 , in pmol). The sampling time is set to 5 min. The system can be represented with the following NARX state space:

$$y(k+1) = f(x(k), u(k)) + e(k), \quad (1)$$

where $u(k) = (u_1(k), u_2(k))$, $e(k) \in \mathbb{R}^{n_y}$ is the process noise and $x \in \mathbb{R}^{n_x}$ is the regression state $x(k) = (y(k), \dots, y(k - n_a), u_1(k - 1), \dots, u_1(k - n_b), u_2(k - 1), \dots, u_2(k - n_c))$, where $n_a, n_b, n_c \in \mathbb{N}_0$ are the memory horizons for the glucose, for the meals and for the basal insulin, respectively. A data set of $N_{\mathcal{D}}$ observations, denoted $\mathcal{D} = \{([w]_k, [y]_{k+1})\}$, for $k = 1, \dots, N_{\mathcal{D}}$ is collected, where $w = (x, u_1, u_2) \in \mathbb{R}^{n_w}$.

A. Componentwise Hölder Kinky Inference (CHoKI)

KI is a class of learning approaches that includes Lipschitz interpolation, which is a technique based on Lipschitz continuity of the function desired to be learned. There exists a more generalized extension, named Hölder continuity [19].

Definition 1. A function $f : \mathcal{W} \rightarrow \mathcal{Y}$ is Hölder continuous if there exist two real constants $L \geq 0$ and $0 < p_l \leq 1$ such that, for all $w_1, w_2 \in \mathcal{W}$,

$$\|f(w_1) - f(w_2)\| \leq L \|w_1 - w_2\|^{p_l}, \quad (2)$$

where L represents the smallest Lipschitz constant and p_l is called the Hölder exponent, $\mathcal{W} \subseteq \mathbb{R}^{n_w}$ is the input space and $\mathcal{Y} \subseteq \mathbb{R}^{n_y}$ is the output space.

In the case of $p_l = 1$, it means to have Lipschitz continuity. In [15], the Hölder constants L and p_l are replaced by the matrices \mathcal{L} and \mathcal{P} , to build the Componentwise Hölder Kinky Inference (CHoKI) method. The aim of the CHoKI is to consider the effect that the variations of each regressor component has on the output. This is based on the componentwise Hölder continuity, defined as follows [15].

Definition 2. Given the matrices \mathcal{L} and $\mathcal{P} \in \mathbb{R}^{n_y \times n_w}$, a function $f : \mathcal{W} \rightarrow \mathcal{Y}$ is componentwise \mathcal{L} - \mathcal{P} -Hölder continuous if $\forall w_1, w_2 \in \mathcal{W}$ and $\forall i \in \mathbb{I}_1^{n_y}$

$$|f(w_1) - f(w_2)| \leq \mathfrak{d}_{\mathcal{L}}^{\mathcal{P}}(|w_1 - w_2|), \quad (3)$$

where

$$\mathfrak{d}_{\mathcal{L}}^{\mathcal{P}}(w) := \left(a : [a]_i = \sum_{j=1}^{n_w} [\mathcal{L}]_{i,j} [w]_j^{[\mathcal{P}]_{i,j}}, \forall i \in \mathbb{I}_1^{n_y} \right). \quad (4)$$

Then, assuming that the function f is Hölder continuous and given a data set \mathcal{D} of $N_{\mathcal{D}}$ inputs/outputs observations, the CHoKI predictor for a query $q_w \in \mathbb{R}^{n_w}$ is defined as:

$$\hat{f}(q_w; \Theta, \mathcal{D}) = \frac{1}{2} \min_{i=1, \dots, N_{\mathcal{D}}} ([\tilde{y}]_i + \mathfrak{d}_{\mathcal{L}}^{\mathcal{P}}(|q_w - [w]_i|)) + \frac{1}{2} \max_{i=1, \dots, N_{\mathcal{D}}} ([\tilde{y}]_i - \mathfrak{d}_{\mathcal{L}}^{\mathcal{P}}(|q_w - [w]_i|)), \quad (5)$$

where $\Theta = \{\mathcal{L}, \mathcal{P}\}$. The matrices \mathcal{L} and \mathcal{P} can be found from the data, solving an offline optimization problem [15].

A new output $\hat{y}(k+1) = \hat{f}(w(k); \Theta, \mathcal{D})$ can be estimated applying (5) and the prediction model can be formulated with the following state-space:

$$\begin{aligned} \hat{x}(k+1) &= \hat{F}(x(k), u_1(k), u_2(k)) \\ \hat{y}(k) &= M\hat{x}(k) \end{aligned} \quad (6)$$

where $\hat{F}(x(k), u_1(k), u_2(k)) = (\hat{f}(x(k), u_1(k), u_2(k)), y(k), \dots, y(k - n_a + 1), u_1(k), \dots, u_1(k - n_b + 1), u_2(k), \dots, u_2(k - n_c + 1))$ and $M = [I_{n_y}, 0, \dots, 0]$.

B. CHoKI implementation for T1D patient

The collection of the data \mathcal{D} is required to apply the CHoKI learning method. This is a fundamental step since the quality of the data will affect the CHoKI predictions and thus the controller performance. This is done by exploiting the UVA/Padova simulator, making several simulations with various virtual adult T1D patients. In particular, to have an appropriate spatial distribution of the insulin-glucose points, different values of the initial BG, of the basal insulin and of the meals amounts (with the bolus injected 20 min after the meal starts) were simulated. Moreover, to obtain more realistic behaviors, some random noises were added. Namely, the virtual typical commercial CGM was selected as a sensor, with auto-regressive noise with inverse Johnson transform distribution. For the virtual pump, its noise has a Gaussian distribution, with 0 pmol mean and 0.1 standard deviation. The meal carbohydrates estimation has a noise with normal distribution, with 30% of the meal amount as standard deviation. Once the data are collected, they have to be correctly shaped to be used inside the CHoKI (i.e. w), which means that the model orders have to be found. In this case, the considered orders are $n_a = 5$, $n_b = 9$ and $n_c = 3$. They are identified through a cross-validation procedure, choosing the combination with the lowest mean squared error between the predictions and the real values, but looking at the model complexity, to avoid the risk of overfitting.

The hyperparameters $\Theta = \{\mathcal{L}, \mathcal{P}\}$ have to be estimated, to get $\hat{f}(q_w; \Theta, \mathcal{D})$, and the same procedure explained in [15, Section B] is followed. In this case, the optimization problem is set to obtain just the values of \mathcal{L} , since the matrix \mathcal{P} is assumed to be $\mathcal{P} = \mathbb{1}_{n_y \times n_w}$. Moreover, to highlight the

TABLE I
MPC SETTINGS

Adult	u_{ref} [pmol]	$N_{\mathcal{D}}$	$[L_a; L_b; L_c]$	μ [mg/dL]	N_c	ϵ
#1	122.38	4769	[0.74; 5.46; 0.29]	14.83	3	10
#2	134.89	4946	[4.89; 3.96; 0.09]	10.19	1	20
#3	149.97	4985	[0.71; 5.45; 0.09]	9.29	3	10
#5	91.83	4149	[0.84; 5.52; 0.44]	13.91	3	5
#6	190.22	5334	[4.72; 3.52; 0.09]	11.27	1	1
#8	105.83	4698	[1.08; 5.84; 0.1]	7.8	3	1
#9	94.59	3976	[1.13; 4.09; 0.09]	11.63	2	1
#10	124.86	4961	[3; 2; 0.09]	10.1	1	20

effect that each input in the regressor has on the output, only three values of \mathcal{L} are estimated. Which means to have $\mathcal{L} = [L_a \mathbb{1}_{n_a}; L_b \mathbb{1}_{n_b}; L_c \mathbb{1}_{n_c}]$, where $L_a \in \mathbb{R}$ is for the glucose part, $L_b \in \mathbb{R}$ for the meals and $L_c \in \mathbb{R}$ for the basal insulin. This procedure is done separately for all the analyzed subjects, using the corresponding initial data set \mathcal{D} to obtain the customized matrix.

Once the optimization problem is solved for all the subjects and the \mathcal{L} are obtained, unseen data sets are used to validate the models. A further analysis was performed to check the models' ability to predict glucose values according to the given inputs correctly. The resulting \mathcal{L} and the values u_{ref} are reported in Table I, for each virtual subject.

III. CHOKI-BASED ROBUST MPC

In this section, the MPC is designed with the CHoKI learning method, exploited to obtain open-loop glucose predictions, allowing to solve the constrained optimization problem at each time instant. According to what is explained in [15], to guarantee the MPC robustness against possible differences among the CHoKI predictions and the real values, the output constraints are tightened according to the propagation of these errors. This way, the system in closed-loop with the proposed controller is proved to be Input-to-State Stable (ISS) [15, Theorem 3].

In this case, the goal of the control problem is to drive and maintain the BG level inside the desired euglycemic zone. This objective has to be reached fulfilling all the desired inputs and output constraints. Namely, the glucose level should be maintained in the set

$$\mathcal{Y} = \{y : 55 \leq y \leq 300 \text{ mg/dL}\} \quad (7)$$

in order to avoid extreme hyper- or hypoglycemic conditions. The basal insulin u_2 is the control action and its amounts have to be inside the set $\mathcal{U} = \{u : 0 \leq u \leq 500 \text{ pmol}\}$.

A. Control and prediction horizons

The control horizon N_c is chosen according to the tightened constraints, which are computed once and offline (see Section IV-A). N_c is the maximum value that allows having a non-empty set of constraints, but also with a meaningful range according to the problem. To improve the controller's predictive ability and to increase the domain of attraction, a prediction horizon (N_p) larger than the control one is chosen, $N_p > N_c$.

For this reason, a local control law is required to compute the inputs from N_c to N_p and, in this work, the Linear Quadratic Regulator (LQR) is exploited on the linearized system $x(k+1) = Ax(k) + Bu(k)$, where $u = (u_1, u_2)$. In particular, the control law will be $u = K(\bar{x} - x) + \bar{u}$, where (\bar{x}, \bar{u}) is an equilibrium point around which the system $\hat{F}(x, u)$ is linearized and $K \in \mathbb{R}^{n_u \times n_x}$ is the LQR control gain. The equilibrium state \bar{x} contains $\bar{y} = 120 \text{ mg/dL}$ as glucose and $\bar{u} = (0, u_{\text{ref}})$. The matrices $A \in \mathbb{R}^{n_x \times n_x}$ and $B \in \mathbb{R}^{n_x \times n_u}$ of the linearized model are numerically computed with the CHoKI, using the input-output data. Thus, each element $[A]_{j,i}$ is given by

$$[A]_{j,i} = \frac{\partial[\hat{F}]_j}{\partial[x]_i} = \frac{[\hat{F}]_j([\bar{x}]_i + \epsilon) - [\hat{F}]_j([\bar{x}]_i - \epsilon)}{2\epsilon}, \quad (8)$$

where ϵ is different for each subject (see Table I). In the same way, each element of B is given by $[B]_{j,i} = \frac{\partial[\hat{F}]_j}{\partial[u]_i}$. Note that $[A]_{1,1} = \frac{\partial[y]_{k+1}}{\partial[y]_k}$ and $[B]_{1,1} = \frac{\partial[y]_{k+1}}{\partial[u_1]_k}$.

B. Constraints tightening (CHoKI-based MPC)

The estimation error must be considered in the design of the controller, thus, the constraints are tightened according to the maximum possible prediction error. The set of restricted output constraints along the control horizon is given by

$$[\mathcal{Y}]_j = \mathcal{Y} \ominus [\mathcal{R}]_j, \quad j = 1, \dots, N_c. \quad (9)$$

Where $[\mathcal{Y}]_0 = \mathcal{Y}$ (in (7)) and $[\mathcal{R}]_j$ are the reachability sets that account for the possible deviation of the predictions from the real system, computed as in [15, Section III-A]. Briefly, the maximum absolute error obtained with the validation data set is $\mu \in \mathbb{R}^{n_y}$ and satisfy $|y(k+1) - \hat{y}(1|k)| \leq \mu$. The difference between a prediction at time step $k+j$ given the measurement at time step k and the prediction at that time step given the measurement at time $k+1$, for the same sequence of control inputs, is bounded by the sets $|\hat{y}(j|k) - \hat{y}(j-1|k+1)| \in [\mathcal{M}]_j \subseteq \mathbb{R}^{n_y}$ and $|\hat{w}(j|k) - \hat{w}(j-1|k+1)| \in [\mathcal{G}]_j \subseteq \mathbb{R}^{n_w}$, where $\sigma(j) = \max(1, j - n_a)$. The reachability sets are defined as $[\mathcal{R}]_j = \{y : |y| \in [\mathcal{M}]_j\}$ for all $j \in \mathbb{I}_1^{N_c}$. The sets $[\mathcal{M}]_j$ and $[\mathcal{G}]_j$ are boxes that can be calculated by the simple recursion $[c]_j = \mathfrak{D}_{\mathcal{L}}^P([d]_{j-1})$ and $[d]_j = ([c]_j, \dots, [c]_{\sigma(j)}, 0, \dots, 0)$, with $[c]_1 = \mu$, where μ is the prediction error bound, and, thus, $[\mathcal{R}]_j = \mathbb{B}([c]_j)$ [15].

In this case, due to the T1D complexity, the reachability sets \mathcal{R} are too big, ending with a small control horizon. Moreover, the constraints are too tight, which leads to possible infeasibilities due to values outside the ranges. For these reasons, a less conservative strategy is proposed in this paper, employing stochastic constraints [17].

IV. CHOKI-BASED STOCHASTIC MPC

In this section, a brief description of the chance constraints theory applied to the stochastic MPC is reported [17]. This method allows a small probability of constraints violation, taking into consideration the probabilistic description of the uncertainty. This could face the infeasibilities, due to possible values outside the tightened constraints. This means having

less conservative tightening, which leads to an increased region of attraction without changing the prediction horizon.

In [17], the predicted state trajectory of the system is decomposed into its deterministic and stochastic components: $\hat{x}(j|k) = \hat{z}(j|k) + \hat{e}_x(j|k)$, $j \in \mathbb{I}_0^{N_c-1}$, given a finite control horizon N_c . Where $\hat{z} \in \mathbb{R}^{n_x}$ represents the evolution of the nominal (deterministic) model and $\hat{e}_x \in \mathbb{R}^{n_x}$ represents the evolution of the stochastic component of the state.

The state constraints $x(j|k) \in \mathcal{X}$ can be stated in a probabilistic way, as $\mathbb{P}\{x(j|k) \in \mathcal{X}\} \geq 1 - \varepsilon$. Which means that the state constraints are satisfied with a probability higher than $1 - \varepsilon$, where ε is the probability of violating the state constraint. Then, they are rewritten component-wise as

$$\mathbb{P}\{[A_x]_i x(j|k) \leq [b_x]_i\} \geq 1 - [\varepsilon]_i, \quad i \in \mathbb{I}_1^p, j \in \mathbb{I}_1^{N_c} \quad (10)$$

and these chance constraints are satisfied if the nominal system satisfies the constraints $z(j|k) \in \tilde{\mathcal{X}}_j$, with

$$\tilde{\mathcal{X}}_j = \{z \in \mathbb{R}^{n_x} | A_x z \leq \eta_j\}, \quad j \in \mathbb{I}_1^{N_c}. \quad (11)$$

Where η_j is given by

$$[\eta_j]_i = \max_{\eta} \quad (12a)$$

$$\text{s.t. } \mathbb{P}_k\{\eta \leq [b_x]_i - [A_x]_i e_x(j|k)\} \geq 1 - [\varepsilon]_i \quad (12b)$$

for $i \in \mathbb{I}_1^p$. Where $A_x \in \mathbb{R}^{p \times n_x}$, $b_x \in \mathbb{R}^p$, p is the number of linear constraints that defines the set \mathcal{X} , $\varepsilon \in [0, 1]^p$ and $[\varepsilon]_i$ is the probability of violating the linear state constraint i [20].

In this paper, the stochastic constraint tightening is implemented exploiting the available measurements of the error (i.e. the difference among the real values and the predictions made with the CHoKI), according to the sampling approach presented in [17, Section V], computing

$$[\eta_j]_i = [b_x]_i - q_{1-r/N_s}. \quad (13)$$

The number of the samples for which the constraints do not hold is r :

$$r \leq \varepsilon_u N_s - \sqrt{2\varepsilon_u N_s \ln \frac{1}{\beta}}, \quad r \geq \varepsilon_l N_s - 1 + \sqrt{3\varepsilon_l N_s \ln \frac{2}{\beta}},$$

where $N_s = 1143$ is the total number of samples, $\varepsilon \in [\varepsilon_l, \varepsilon_u]$ and q_{1-r/N_s} is the $(1 - r/N_s)$ -quantile of the set $\{[A_x]_i e_x^l(j|k)\}_{l=1, \dots, N_s}$. In our case, the $(1 - r/N_s)$ -quantile is computed on the truncated uncertainty distribution obtained through the CHoKI, at each step. Note that the satisfaction of the chance constraints holds with a confidence $1 - \beta = 95\%$ (i.e. $\varepsilon_l = 0.095$ and $\varepsilon_u = 0.105$), since the constraints are obtained directly from the data, with the sampling approach. Thus, the solution to the sampled program is equal to the chance-constrained one with confidence $1 - \beta$.

A. Constraints tightening (CHoKI-based stochastic MPC)

As in [17], the system describing a T1D patient can be split into its deterministic and stochastic components, (1). The output constraints have to be tightened. The computation is done once and offline, to obtain y_{\min} and y_{\max} (i.e. η_j from (13)), given the evolution of the uncertainty, to have

$$[\mathcal{Y}']_j = \{y : y_{\min}(j) \leq y \leq y_{\max}(j)\}. \quad (14)$$

The propagation of the error is obtained computing $[c]_j$ and $[d]_j$ at each step, as reported in Section III-B. The main difference is that since in this case the constraints tightening is based on the probability distribution of the errors, the computation is done considering all the uncertainty values, to get the distribution at each step. Once these are obtained, each mean is subtracted from all the values to fit a normal distribution with zero mean (since in the computation of $[c]_j$ and $[d]_j$ the propagation of the error is in absolute value) and this is then truncated at the value corresponding to the 90th percentile (with $\varepsilon = 0.1$, because of the 10% probability of constraints violation). Then, the $(1 - r/N_s)$ -quantile is computed and the entire procedure is repeated for all the considered virtual subjects. The values of the 90th percentiles at the first prediction step are the μ reported in Table I.

The values of the tightened constraints affect also the choice of the control horizons N_c (reported in Table I), for each virtual subject. While the prediction horizon is set to $N_p = 12$ for all (to reach 60 min of predictions).

B. Optimization problem (CHoKI-based stochastic MPC)

The optimization problem is set as follows:

$$\min_{u_2, y_a, \delta_{\text{hyper}}, \delta_{\text{hypo}}} V_N(\hat{x}, u; \Theta, \mathcal{D}) \quad (15a)$$

$$\text{s.t. } \hat{x}(0|k) = x(k) \quad (15b)$$

$$\hat{x}(j+1|k) = \hat{F}(\hat{x}(j|k), u_1(j), u_2(j)), j \in \mathbb{I}_0^{N_c-1} \quad (15c)$$

$$\hat{x}(j+1|k) = \hat{F}(\hat{x}(j|k), K(\bar{x} - x(j)) + \bar{u}), j \in \mathbb{I}_{N_c}^{N_p-1} \quad (15d)$$

$$\hat{y}(j|k) = M\hat{x}(j|k), \quad u_2(j) \in \mathcal{U}, \quad j \in \mathbb{I}_0^{N_p-1} \quad (15e)$$

$$\hat{y}(j|k) \in [\mathcal{Y}]_j, \quad j \in \mathbb{I}_0^{N_c-1} \quad (15f)$$

$$\hat{y}(j|k) \in [\mathcal{Y}]_{N_c}, \quad j \in \mathbb{I}_{N_c}^{N_p-1} \quad (15g)$$

$$u_1(j) = 0, \quad j \in \mathbb{I}_1^{N_p-1} \quad (15h)$$

$$70 - \delta_{\text{hypo}} \leq y_a \leq 140 + \delta_{\text{hyper}} \quad (15i)$$

$$\delta_{\text{hyper}} \geq 0, \quad \delta_{\text{hypo}} \geq 0 \quad (15j)$$

where (15h) is used since the meals are not predictable.

The cost function is built in this way:

$$V_N(\hat{x}, u; \Theta, \mathcal{D}) = V_{N_c} + V_{N_p} + V_s + \lambda V_p,$$

Where the first term is the stage cost V_{N_c} , along the control horizon:

$$V_{N_c} = \sum_{j=0}^{N_c-1} \|\hat{y}(j|k) - y_a\|_Q^2 + \|u_2(j) - u_{\text{ref}}\|_R^2 \quad (16)$$

where the set-point y_a is an auxiliary optimization variable, which is constrained to be inside the interval [70, 140] and needed for the implementation of the MPC in a zone control fashion. Since some slack variables δ_{hypo} , δ_{hyper} are added to the constraints of y_a (15i), a stationary cost V_s is created:

$$V_s = p_{\text{hyper}} \delta_{\text{hyper}}^2 + p_{\text{hypo}} \delta_{\text{hypo}}^2, \quad (17)$$

with asymmetric weights, $p_{\text{hypo}} > p_{\text{hyper}}$, to represent that hypoglycemia is more dangerous than hyperglycemia [8].

Similarly to the stationary cost, from N_c to $N_p - 1$, the cost V_{N_p} is given by

$$V_{N_p} = \sum_{j=N_c}^{N_p-1} \|\hat{y}(j|k) - y_a\|_Q^2. \quad (18)$$

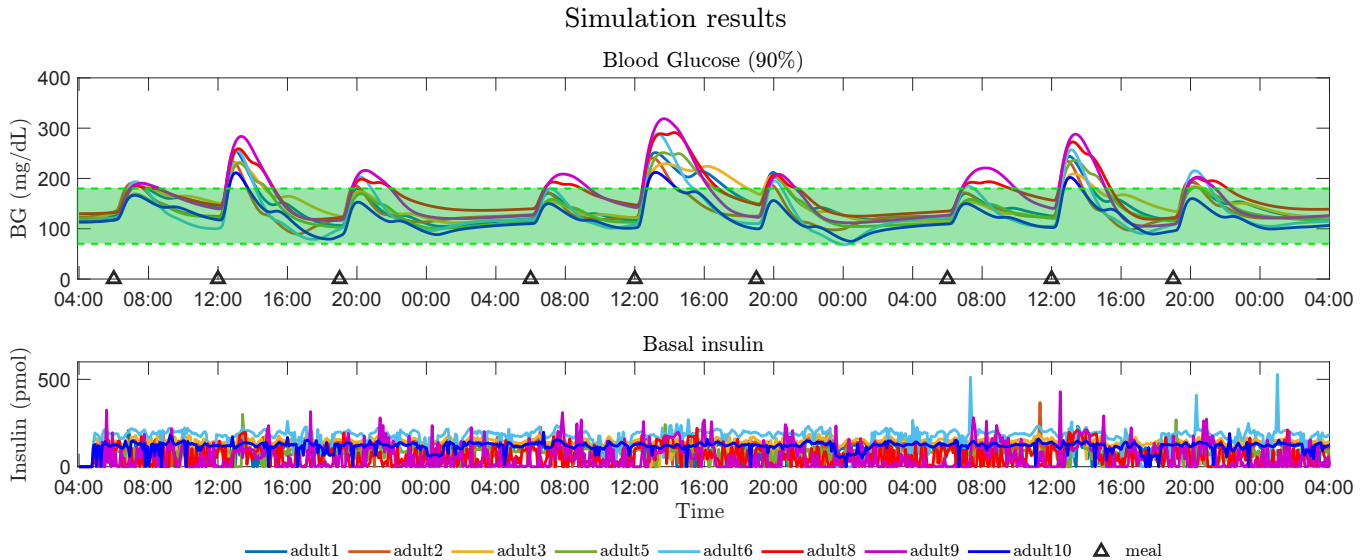


Fig. 1. Each line represents a specific virtual patient. In the upper graph, the lines represent the BG trend, the black triangles depict the meals time and the green zone is the safe range (i.e. 70-180 mg/dL). In the lower graph, the basal insulin injections.

The terminal cost V_P penalizes the difference between the last state and the reference state (x_{ref} , which contains y_a , no meals and u_{ref}):

$$V_P = \|\hat{x}(N_p|k) - x_{\text{ref}}\|_P^2, \quad (19)$$

where P is the solution to the Riccati equation, given the LQR control gain K . The terminal cost is usually employed to guarantee the MPC stability and it is weighted by a factor $\lambda > 0$, since no terminal constraint is considered [21]. Moreover, several combinations of the weights were tested and the definitive ones are the following: $R = 10$, $p_{\text{hypo}} = 1 \cdot 10^7$, $p_{\text{hyper}} = 1 \cdot 10^6$, $\lambda = 10$ and $Q = 1$, except for Adult 8 and 9, for whom $Q = 100$.

The aim is to create a customized controller, which means that for each of the analyzed virtual patients is set a personalized optimization problem, with the corresponding values.

V. SIMULATIONS AND RESULTS

In this section the proposed customized MPC with stochastic constraints is applied as control algorithm of the virtual AP in the UVA/Padova simulator. The controller is tested on the virtual T1D adults, through three-day simulations, with the following 15 min duration meals each day: 40 g of carbohydrates at 06:00am, 100 g at 12:00pm and 60 g at 07:00pm; and the boluses, computed by the simulator, are injected 20 min after the meal starts. The simulations settings are the same as the ones used for the data collection.

The results of the simulations are displayed in Figure 1, where the upper graph represents the BG outcomes, while the lower graph shows the basal insulin injections computed by the proposed MPC. The BG values are mainly inside the euglycemic range (i.e. the green zone), except for some higher values that are caused by the ingestion of the carbohydrates (note that the black triangles depict the meals).

Looking at the BG trends may be not enough and indeed other important tools are considered for the evaluation of the quality of the insulin-glucose management: the Control-Variability Grid Analysis (CVGA) and the Time In Range (TIR). The former is a graphical representation of the simulation "worst condition", with the minimum BG value on the x -axis and the maximum one on the y -axis and where each dot represents a subject [22]. The latter shows the percentages of time a patient spends in each specific BG range. The CVGA results are shown in Figure 2, looking at the dots. These are satisfying since all the dots are inside the safe zones A and B. The TIR results are reported in the upper part of Table II. The TIR requirements are mostly satisfied since the subjects stay between 70 and 180 mg/dL for more than the 70% of the simulation time, according to the American Diabetes Association requirements. An exception occurs for adults 8 and 9, who are slightly more than 5% over 250 mg/dL and adult 8 also has TIR equal to 69%. However, they always fulfill the time requirements for the hypoglycemic ranges, which was the main goal, due to its dangerousness.

In Figure 2 and in the lower part of Table II are reported the CVGA (see the squares) and TIR results of the continuous basal therapy provided by the simulator, to make a comparison. The benefit of the proposal, particularly in the management of hypoglycemic conditions, is clear. For example, looking at the CVGA, the virtual patients adult 5 and adult 9 pass from the Lower D zone to the Upper B zone (green and purple dots and squares in Figure 2, respectively), which means that the minimum BG value is increased.

VI. CONCLUSION

A CHoKI-based MPC with stochastic constraints tightening is proposed as control algorithm of the AP, with the aim of driving and maintaining the T1D patients' BG values inside the euglycemic range, updating the basal insulin injec-

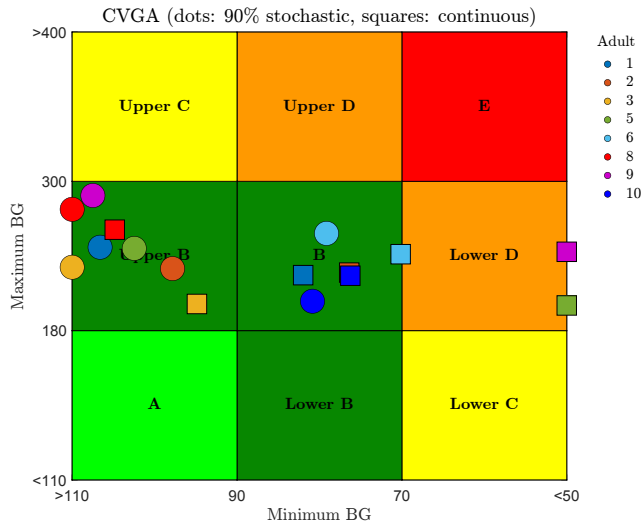


Fig. 2. CVGA result with BG measurements. Dots: 90% stochastic case. Squares: continuous basal case.

TABLE II
TIR PERCENTAGES

	Adult	< 54 mg/dL	54-70 mg/dL	70-180 mg/dL	180-250 mg/dL	> 250 mg/dL	
Proposed controller	# 1	0%	0%	84%	15%	1%	
	# 2	0%	0%	90%	10%	0%	
	# 3	0%	0%	81%	19%	0%	
	# 5	0%	0%	85%	14%	1%	
	# 6	0%	1%	84%	12%	3%	
	# 8	0%	0%	69%	25%	6%	
	# 9	0%	0%	70%	23%	7%	
	# 10	0%	0%	95%	5%	0%	
	Constant insulin therapy	# 1	0%	0%	92%	8%	0%
		# 2	0%	2%	91%	7%	0%
# 3		0%	0%	94%	6%	0%	
# 5		14%	7%	75%	4%	0%	
# 6		0%	2%	87%	10%	1%	
# 8		0%	0%	77%	18%	5%	
# 9		6%	7%	78%	8%	1%	
# 10		0%	0%	91%	9%	0%	

tions amount every 5 min. The application of the proposed controller to the virtual patients of the UVA/Padova simulator is presented. The results are quite promising and the main outcome is that it reduces the hypoglycemic events, which is fundamental due to their dangerousness. This is possible thanks to the CHoKI ability to forecast future glucose values, which allows the MPC to find the optimal insulin amounts, to reach and maintain the BG goal, respecting the imposed constraints. Future work will be focused on the study of recursive feasibility and stability of the proposed controller.

REFERENCES

[1] A. Katsarou, S. Gudbjörnsdóttir, A. Rawshani, D. Dabelea, E. Bonifacio, B. J. Anderson, L. Jacobsen, D. A. Schatz, and A. Lernmark, "Type 1 diabetes mellitus," *Nature Reviews Disease Primers*, vol. 3(1), 2017.

[2] Rawlings, J. Blake, and D. Q. Mayne, *Model predictive control: Theory and design*. Nob Hill Pub., 2009.

[3] S. Del Favero, C. Toffanin, L. Magni, and C. Cobelli, "Deployment of modular mpc for type 1 diabetes control: the italian experience 2008–2016," in *The Artificial Pancreas*, pp. 153–182, Elsevier, 2019.

[4] C. Toffanin, M. Messori, F. Di Palma, G. De Nicolao, C. Cobelli, and L. Magni, "Artificial pancreas: model predictive control design from clinical experience," 2013.

[5] R. Hovorka, V. Canonico, L. J. Chassin, U. Haueter, M. Massi-Benedetti, M. O. Federici, T. R. Pieber, H. C. Schaller, L. Schaupp, T. Vering, *et al.*, "Nonlinear model predictive control of glucose concentration in subjects with type 1 diabetes," *Physiological measurement*, vol. 25, no. 4, p. 905, 2004.

[6] B. Kovatchev, "Automated closed-loop control of diabetes: the artificial pancreas," *Bioelectronic Medicine*, vol. 4, no. 1, pp. 1–12, 2018.

[7] D. Boiroux, V. Bátorá, M. Hagdrup, S. L. Wendt, N. K. Poulsen, H. Madsen, and J. B. Jørgensen, "Adaptive model predictive control for a dual-hormone artificial pancreas," *Journal of Process Control*, vol. 68, pp. 105–117, 2018.

[8] P. Abuin, P. S. Rivadeneira, A. Ferramosca, and A. H. González, "Artificial pancreas under stable pulsatile mpc: Improving the closed-loop performance," *Journal of Process Control*, vol. 92, pp. 246–260, 2020.

[9] P. Soru, G. De Nicolao, C. Toffanin, C. Dalla Man, C. Cobelli, L. Magni, A. H. Consortium, *et al.*, "Mpc based artificial pancreas: strategies for individualization and meal compensation," *Annual Reviews in Control*, vol. 36, no. 1, pp. 118–128, 2012.

[10] R. Gondhalekar, E. Dassau, and F. J. Doyle III, "Periodic zone-mpc with asymmetric costs for outpatient-ready safety of an artificial pancreas to treat type 1 diabetes," *Automatica*, vol. 71, pp. 237–246, 2016.

[11] A. H. González, P. S. Rivadeneira, A. Ferramosca, N. Magdelaine, and C. H. Moog, "Impulsive zone mpc for type i diabetic patients based on a long-term model," *IFAC-PapersOnLine*, vol. 50, no. 1, pp. 14729–14734, 2017.

[12] A. H. González, P. S. Rivadeneira, A. Ferramosca, N. Magdelaine, and C. H. Moog, "Stable impulsive zone model predictive control for type 1 diabetic patients based on a long-term model," *Optimal Control Applications and Methods*, vol. 41, no. 6, pp. 2115–2136, 2020.

[13] D. Shi, E. Dassau, and F. J. Doyle, "Adaptive zone model predictive control of artificial pancreas based on glucose-and velocity-dependent control penalties," *IEEE Transactions on Biomedical Engineering*, vol. 66, no. 4, pp. 1045–1054, 2018.

[14] I. Hajizadeh, M. Rashid, and A. Cinar, "Plasma-insulin-cognizant adaptive model predictive control for artificial pancreas systems," *Journal of process control*, vol. 77, pp. 97–113, 2019.

[15] J. M. Manzano, D. Muñoz de la Peña, J.-P. Calliess, and D. Limon, "Componentwise Hölder Inference for Robust Learning-Based MPC," *IEEE transactions on automatic control*, vol. 66(11), pp. 5577–5583, 2021.

[16] B. Sonzogni, J. M. Manzano, M. Polver, F. Previdi, and A. Ferramosca, "CHoKI-based MPC for blood glucose regulation in artificial pancreas," *Accepted for publication in the 22nd IFAC World Congress*, 2023.

[17] M. Lorenzen, F. Dabbene, R. Tempo, and F. Allgöwer, "Constraint-tightening and stability in stochastic model predictive control," *IEEE Transactions on Automatic Control*, vol. 62, no. 7, pp. 3165–3177, 2016.

[18] The Epsilon Group, "DMMS.R (Version 1.1) [Software]." Retrieved from <https://tegvirginia.com/>, 2016.

[19] J. M. Manzano, D. Limon, D. Muñoz de la Peña, and J.-P. Calliess, "Robust learning-based MPC for nonlinear constrained systems," *Automatica*, vol. 117, 2020.

[20] A. D'Jorge, B. F. Santoro, A. Anderson, A. H. González, and A. Ferramosca, "Stochastic model predictive control for tracking linear systems," *Optimal Control Applications and Methods*, vol. 41, no. 1, pp. 65–83, 2020.

[21] D. Limon, T. Alamo, F. Salas, and E. F. Camacho, "On the stability of constrained mpc without terminal constraint," *IEEE transactions on automatic control*, vol. 51, no. 5, pp. 832–836, 2006.

[22] L. Magni, D. M. Raimondo, C. Della Man, M. Breton, S. Patek, G. D. Nicolao, C. Cobelli, and B. P. Kovatchev, "Evaluating the efficacy of closed-loop glucose regulation via Control-Variability Grid Analysis," *Journal of diabetes science and technology*, vol. 2(4), pp. 630–635, 2008.